Available online at www.sciencedirect.com
SCIENCE DIRECT
Journal of Sound and Vibration 296 (2006) 757–776
JOURNAL OF SOUND AND VIBRATION
www.elsevier.com/locate/jsvi

A simplified methodology to predict the dynamic stiffness of carbon-black filled rubber isolators using a finite element code

N. Gil-Negrete[a,*], J. Viñolas[a], L. Kari[b]

[a]CEIT and Tecnun (University of Navarra), Department of Applied Mechanics, P° Manuel Lardizabal 15, 20018 San Sebastian, Spain
[b]KTH, Department of Aeronautical and Vehicle Engineering, MWL, SE-10044 Stockholm, Sweden

Received 16 February 2005; received in revised form 31 January 2006; accepted 7 March 2006
Available online 2 June 2006

Abstract

A new and different approach to the inclusion of the amplitude-dependent effect, known as the Fletcher–Gent effect or Payne effect, in a linear viscoelastic rubber material model is presented to predict the dynamic stiffness of filled rubber isolators using a finite element (FE) code. The technique is based on providing a linear viscoelastic model with the adequate material data set, once the dynamic strain amplitude, to which the rubber mount is subjected, is estimated. A generalized Zener model is adopted to describe the frequency-dependent behaviour of the material through the use of hereditary integrals. The dynamic strain amplitude dependence is not modelled through any friction model or plasticity theory, as usually is in literature. It is introduced by considering the frequency-dependent properties of the compound at an adequate strain value, which enforces the estimation of an equivalent strain value. As a first approximation, a quasi-static value is used as the reference value at which material properties should be provided to the linear viscoelastic model. The technique works directly in frequency domain, the dynamic stiffness of the bushing being directly obtained. The methodology is applied to evaluate the dynamic stiffness of a real bushing in working conditions with very satisfactory results. Despite the assumptions made, especially regarding the estimation of the equivalent strain amplitude value, errors of the predictions fall within the limits usually accepted by rubber manufacturers.

1. Introduction

Rubber is, without doubt, the cheapest and the most widely accepted solution when the connection between two parts of a structure, a vehicle or a machine requires a combination of stiffness and vibration isolation. When a source has to be connected to a receiving structure, mounting it upon vibration isolators attains a simple vibration transmission reduction. Elastomeric mounts have long been used to isolate structures from unwanted vibrations, as they can be designed so that desired stiffness characteristics are achieved in all directions for proper vibration isolation.

Despite rubber being so common, knowledge of the material properties among design engineers is often poor. Insufficient knowledge of transmission and damping properties of rubber joints, as well as modelling

*Corresponding author. Tel.: +34 943212800x2249; fax: +34 943213076.
E-mail address: ngil@ceit.es (N. Gil-Negrete).

0022-460X/$ - see front matter © 2006 Elsevier Ltd. All rights reserved.
doi:10.1016/j.jsv.2006.03.038

techniques for rubber isolators, has often forced industry to carry out costly experimental work for optimising the shape, location and volume of the units. A number of design engineers tend to simplify the problem by modelling the isolator through a single linear spring. Values used in the design stage are estimated from quasi-static elastic characteristics and, damping, if considered, is most of the times represented by a unique dashpot of arbitrary parameter. Nonlinear effects of rubber are either not known or ignored.

When rubber is subjected to large quasi-static preloads prior to small-amplitude harmonic excitation, even in the case of unfilled natural rubber, it shows a pronounced progressive stress–strain curve, meaning that elastic behaviour is not linear any more. Furthermore, due to fillers added to rubber mixture to fulfil both vibration isolation and structural specifications, material properties develop nonlinear characteristics. Elastic behaviour might not be considered through a constant Young's modulus, as it becomes strain dependent. On the other hand, dynamic properties of the material are strongly dependent on temperature, frequency and strain amplitude. Thorough reviews of strain amplitude, frequency and temperature effects on mechanical rubber characteristics, based on experimental measurements, are conducted, for example, by Jurado et al. [1], Medalia [2], Dean et al. [3] and Wang [4]. The work by Wang goes even further, presenting theories and observations about why the inclusion of filler alters the linear dynamic stress–strain response of unfilled rubber compounds. Because of its nonlinear characteristics, modelling either the behaviour of a mixture or that of a bushing to predict, at a design stage, its response to excitation becomes a complex issue.

The development of computers and analysis programs has given engineers a new tool in design and construction of elastomeric components, as well as in the prediction of their dynamic behaviour. Computer simulation by finite element (FE) method is becoming increasingly important due to its capability to solve complex problems that are not readily tractable by classical analytical methods. Furthermore, the FE method provides a procedure for analysis of structures of different types of material and arbitrary geometric form. Nevertheless, its accuracy depends on the accuracy to which the elastic and dynamic nature of the design material can be defined.

Historically, the focus of researchers has been to model mathematically one of the dependencies of rubber, while ignoring the other ones. Nonlinear elasticity has received special attention over the years, since early in the 20th century [5–8] till today [9–12], with the proposal of many different strain energy functions that would represent the characteristic and be implemented in commercial FE codes.

As for the dynamic behaviour, time domain viscoelastic models can provide an accurate description of the frequency-dependent behaviour of rubber materials. Quite simple models arise from linear viscoelasticity as early as in the 1960s or 1970s, which have become very popular to represent the behaviour of rubber material in frequency (Refs. [13–16], for example, and discussions by Sjöberg [17] and Gil-Negrete [18]). These viscoelastic models involve combinations of springs and dashpots and a large number of parameters as a sophisticated generalized model must be addressed to accurately represent frequency-dependent effects in a frequency range. For a full three-dimensional case, constitutive equations are formulated through hereditary or convolution integrals. The most interesting such models have been proposed by Lubliner [19], Johnson et al. [20,21], Yang et al. [22] and Simo [23], whose model is also focused on the inclusion of Mullins' effect [24]. Linear multiaxial viscoelasticity is already available in the majority of FE codes.

More recently fractional calculus has been included in the modelling of viscoelasticity, as an alternative approach to obtain good description of frequency-dependent behaviour while reducing the required number of parameters. Although the mathematical history of fractional derivatives goes back to the 17th century [25], its use in the field of viscoelasticity started with Bagley and Torvik [26] in the 1980s. Since then different authors have included fractional derivatives in their models for different applications connected to rubber mounts [18,27–33].

The fractional derivative viscoelastic model is suitable to be used in a structural dynamic analysis and may be implemented into a general-purpose FE code. Time domain formulations are given by Padovan [34] and Enelund et al. [35]. Adolfsson [36] extends Enelund's model to include nonlinear elastic effects. The main drawback of fractional order viscoelasticity is that, nowadays, multiaxial fractional derivative viscoelasticity is not usually included in commercial FE codes, the user being responsible for its implementation through user routines.

Viscoelastic models (both the classical ones and the ones that involve fractional derivatives) are sufficient for representing the behaviour of poorly filled or soft rubbers. Nevertheless, the amplitude dependence, not

described by models of linear viscoelasticity, might be of significance if the material is more heavily filled looking for other properties, such as hardness or abrasion resistance and even higher damping.

One approach to include this effect, also known as the Fletcher–Gent effect [37] or Payne effect [38], in the model of rubber components involves working with nonlinear viscous damping forces [39–42]. Kraus [43] proposes a one-dimensional model of the amplitude dependence, where it is considered to be due to the continuous breaking and reforming of Van der Waals forces between carbon-black aggregates. His model is later used and revised by Ulmer [44].

Nevertheless, the Fletcher–Gent effect is usually denoted as plastic effect [45]. It can be attributed to irreversible slip processes between the filler particles and their plastic deformations [46]. This has motivated to characterize the amplitude-dependent effect through friction elements, which is the idea behind Gregory's [47] or Austrell's [48] models, where several friction chains involving Coulomb friction elements must be connected in parallel to obtain good results. Berg [49] presents a more efficient friction model, showing smoother characteristics than Coulomb friction models with less parameter. Berg's model has successfully been adopted by Sjöberg and Kari [33,50] when simulating vibration isolators. Although interesting due to the reduced number of coefficients that need to be tuned, Berg's model poses a problem when it comes to be adopted for a multiaxial rubber model as it is formulated for a uniaxial case, relating forces and displacements. Implementation in general purpose FE codes does not seem immediate.

Kaliske et al. [46], Austrell et al. [48] and Rabkin et al. [51] have presented friction models suitable for FE codes. Kaliske et al. propose a generalized Prandtl element, formulated analogously to the generalized viscoelastic element, while in Rabkin's work the friction part is defined as a parallel composition of an infinite number of the St. Venant dry friction damper with continuously distributed yield stress. Lion [52] also proposes the use of Prandtl elements, transforming their time-domain response to the frequency domain and calculating the amplitude-dependent storage and loss moduli in closed form. It is interesting to remark the work by Austrell et al, as they implement a generalized Coulomb friction model making use of the Von Mises elastoplasticity already available in FE codes, thus simplifying the implementation of the friction part.

When the aim of the model is the prediction of the dynamic stiffness of filled rubber components the usage of coupled viscoelastic–friction models presents two problems. First of all, the parameters of the model, both for the viscoelastic and friction parts, have to be calibrated from tests conducted on material samples. It has to be determined which tests to conduct and under what conditions and how to fit the coefficients of the model. Secondly, the nonlinear friction models usually force the calculation to be conducted in time domain and results be converted to frequency domain, investing time and computer resources.

In this study a different approach to the inclusion of friction effects in a linear viscoelastic rubber material model is presented to predict the dynamic stiffness of filled rubber isolators using a commercial FE code. The technique is based on providing a linear viscoelastic model with the adequate material data set, once the dynamic strain amplitude, to which the rubber mount is subjected, is estimated. This enforces the calculation of an equivalent strain value.

The procedure, running in frequency domain, presents an approximate, but fast, easy to implement and innovative method to consider the dynamic nonlinearities of rubber mixtures when predicting the dynamic stiffness of bushings using FE codes.

2. Material testing

Dynamic properties of four different natural rubber compounds (filled with two types of carbon black: SRF N-772 and NEGROMEX N-330, the amount of each depending on the desired hardness) have been evaluated through a forced non-resonant simple shear test, following suggestions in ASTM D5992-96 [53]. The sample used is shown in Fig. 1. Measurements are conducted for a frequency range 0–500 Hz and a peak amplitude range 0.01–0.2 mm. Note that the sample proposed for the dynamic measurements is half of the specimen for quasi-static measurements suggested in ISO 1827 [54], which is not suitable for the forced non-resonant dynamic simple shear test in the frequency range of the study. This new configuration overcomes the dynamic problems of the standardized quasi-static sample due to the inertia effect of the two metal parts that connect the four rubber blocks. Its main advantage, compared to other configurations, is that the test set-up is exactly

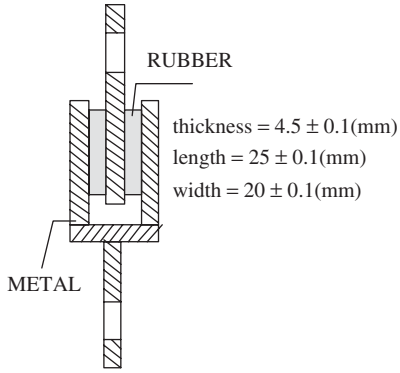

Fig. 1. Simple shear sample proposed for measuring the dynamic properties of rubber material.

the same as for the quasi-static simple shear test. Thus, the same testing machine and clamping devices could be used for both measurements. Furthermore, the election of this mode of deformation (simple shear) seems also very adequate as elastic nonlinearities are reduced. Nevertheless, applied maximum strain level should be sufficiently small to ensure a pure simple shear deformation. If higher strain levels were of interest, the dimensions of the sample should be enlarged to avoid the presence of bending.

Experimental tests have been carried out at Seat Centro Técnico in a SCHENCK, hydropuls High-Frequency Testing Machine VHF 7, with a limit in frequency range of 1000 Hz. Four samples of each compound have been tested to ensure the repetitivity of the results. Furthermore, some initial cycles have been applied to the samples before starting measurements to avoid the stiffening due to Mullins' effect [24].

When a sinusoidal deformation is applied to a rubber, the overall response of the material can be expressed in terms of a complex modulus [18]:

$$G^* = G_1 + jG_2 = G_1(1 + j\tan\delta). \tag{1}$$

In Eq. (1) G_1 is the in phase, storage modulus, and G_2 is the out of phase, loss modulus. The loss angle, related to the damping or hysteretic energy losses of the material, is given by $\tan\delta = G_2/G_1$. Both the modulus $|G^*|$ and the loss angle δ of natural rubber compounds are very dependent on various parameters, mainly frequency, dynamic strain amplitude, temperature and preload. Influence of frequency and strain amplitude are presented here. In the figures described below, specimens compounded of four different rubber mixtures are compared. All of them are natural rubber and they are classified by their hardness in Shore A degrees scale [55]: Shore A 40, Shore A 50, Shore A 60 and Shore A 70. A higher degree means a higher content of carbon-black filler.

Fig. 2 shows that $|G^*|$ increases with hardness and slightly with frequency in the region of interest. Nevertheless, it is important to point out that a "jump" has been observed to exist between the quasi-static and the dynamic (even at low frequencies) value of $|G^*|$ (see Table 1). For unfilled rubbers the "jump" might not be important (less than 25%), but as the amount of filler increases it becomes more noticeable. The reason for it is not yet understood, although it has also been observed by other researchers [56].

Natural rubber displays a larger dynamic modulus at small amplitudes than at larger dynamic strain amplitudes (Fig. 3). The effect is more pronounced as the amount of fillers is increased in the compound, so that unfilled rubbers could be considered not dependent on amplitude at all. The main reason of this effect is believed to be the breakdown of interactions within the filler and between the filler and the rubber matrix [38]. At small amplitudes, the dynamic modulus is large due to the intact filler structure. As the amplitude increases the structure breaks, resulting in dynamic modulus decrease.

The breaking of filler structure, however, described as frictional behaviour, causes an increment in the damping (Fig. 4). The increase of the loss factor is not maintained in all range of amplitudes: the curve of loss angle versus amplitude smoothens at large amplitudes. It seems to be related with remaining polymer chains and hydrodynamic effects [38].

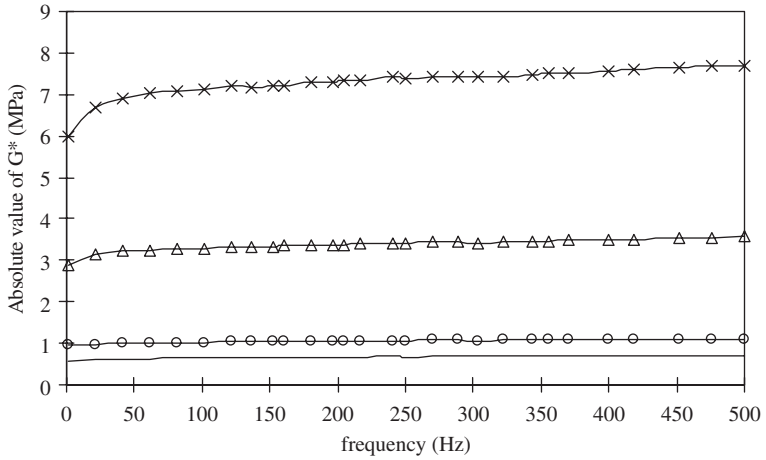

Fig. 2. Absolute value (magnitude) of the complex shear modulus (MPa). Comparison among rubbers of different hardness: — Shore A 40; ○ Shore A 50; △ Shore A 60; × Shore A 70. Applied dynamic strain amplitude of 0.02 mm. Room temperature.

Table 1
Comparison between the quasi-static and dynamic $|G^*|$ (Pa) at room temperature and 0.05 mm amplitude

Shore A	$\|G^*\|$(Pa)–$f = 1$ Hz	G stat (Pa)[a]	$\|G^*\|/G$ stat
40	5.58E + 05	4.49E + 05	1.24
50	9.54E + 05	6.24E + 05	1.53
70	3.90E + 06	1.65E + 06	2.36

[a]Quasi-static values have been obtained by standardised quasi-static tests and considering linear relationship between stress and strain, which is not completely true due to the nonlinearity of material.

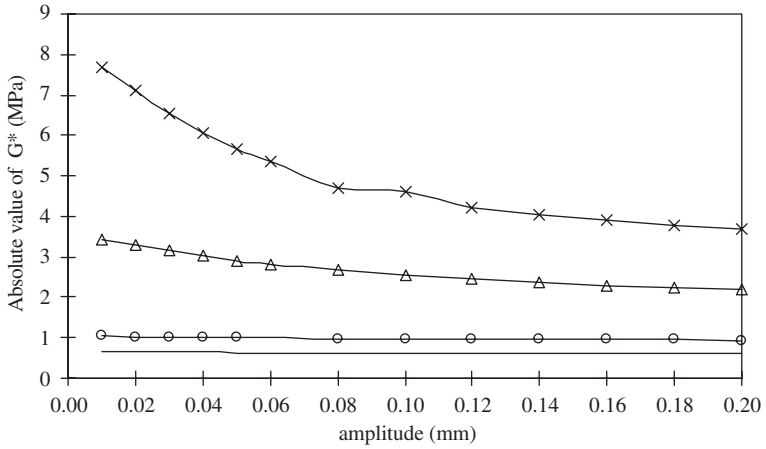

Fig. 3. Amplitude dependence of the absolute value (magnitude) of the complex shear modulus (MPa). Comparison among rubbers of different hardness: — Shore A 40; ○ Shore A 50; △ Shore A 60; × Shore A 70. Frequency: 102 Hz. Room temperature.

3. Description and implementation of the procedure proposed

Fig. 5 shows a generalized Maxwell material model that provides a very good fitting to experimental frequency-dependent data of the material. If a shear strain γ is applied to the uniaxial model presented, the

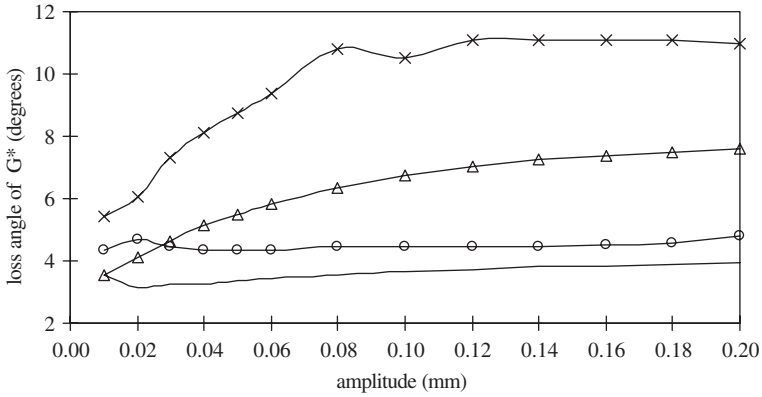

Fig. 4. Amplitude dependence of the loss angle of the complex shear modulus (degrees). Comparison among rubbers of different hardness: — Shore A 40; ○ Shore A 50; △ Shore A 60; × Shore A 70. Frequency: 102 Hz. Room temperature.

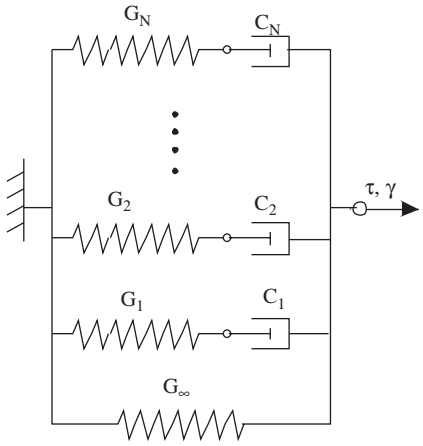

Fig. 5. Schematic representation of the generalized Maxwell model.

total stress will be the sum of stresses in each Maxwell element alone, plus the stress in the solitary spring of stiffness G_∞:

$$\tau(t) = \tau_\infty + \sum_{i=1}^{N} \tau_i^e = \tau_\infty + \sum_{i=1}^{N} \tau_i^v \rightarrow \begin{cases} \tau_i^e = G_i(\gamma - \gamma_i^v), \\ \tau_i^v = C_i \dot{\gamma}_i^v. \end{cases} \tag{2}$$

In Eq. (2) τ_i^e refers to the stress over the spring in chain "i" and τ_i^v to the stress over the dashpot in the same chain. As for y_i^v, it represents the strain over the dashpot "i" and it is solved through the following differential equation, equalling the stresses in the spring and dashpot of chain "i":

$$\tau_i^e = \tau_i^v \rightarrow G_i(\gamma - \gamma_i^v) = C_i \dot{\gamma}_i^v \Rightarrow \dot{\gamma}_i^v = \frac{G_i}{C_i}(\gamma - \gamma_i^v). \tag{3}$$

The behaviour of the viscoelastic models can also be represented in terms of hereditary integrals, a theory first formulated by Boltzmann in 1876 [57]. The theory, based on the Boltzmann superposition principle, uses a convolution integral relation between stress and strain and leads to equations that are more suitable for implementation in FE codes (see Section 3.1). If a shear strain γ is applied to a viscoelastic material, the developed shear stress at time t is characterized by the following convolution integral:

$$\tau(t) = \int_{-\infty}^{t} G(t-\tau)\frac{\mathrm{d}\gamma(\tau)}{\mathrm{d}\tau}\mathrm{d}\tau. \tag{4}$$

For applied strains being zero till $t = 0$, Eq. (4) may also be written in the form:

$$\tau(t) = \gamma(0)G(t) + \int_{0^+}^{t} G(t-\tau)\frac{\mathrm{d}\gamma(\tau)}{\mathrm{d}\tau}\mathrm{d}\tau. \tag{5}$$

Expression (5) may be brought into another (Eq. (6)) through integration by parts and variable transformation:

$$\tau(t) = G_0\gamma(t) + \int_{0^+}^{t} \gamma(\tau)\frac{\mathrm{d}G(t-\tau)}{\mathrm{d}(t-\tau)}\mathrm{d}\tau = \tau_0(t) + \int_{0^+}^{t} \gamma(t-s)\frac{\mathrm{d}G(s)}{\mathrm{d}s}\mathrm{d}s. \tag{6}$$

In all the above equations $G(t)$ represents the time-dependent analogous to the elastic shear modulus G for viscoelastic materials. The shear relaxation modulus is shown in Fig. 6. G_0 and G_∞ are known as the instantaneous and long-term shear relaxation moduli, respectively. The time-dependent shear relaxation modulus can be determined from relaxation tests carried out at material samples.

Frequency domain viscoelasticity can be described applying the Fourier transformation to the expressions that define the time domain viscoelasticity. The shear stress resultant to the application of a time varying shear strain is given by the shear stress relaxation function defined in Eq. (4). However, Fig. 6 shows that the relaxation shear modulus decreases to a finite value. In order to calculate de Fourier transform, it is more convenient to introduce a dimensionless relaxation modulus, such as that of Eq. (7).

$$g(t) = \frac{G(t)}{G_\infty} - 1. \tag{7}$$

Introducing Eq. (7) in Eqs. (4) and (5), they develop the following form (after adequate variable transformation):

$$\tau(t) = G_\infty\gamma(t) - G_\infty\int_0^t g(s)\frac{\mathrm{d}\gamma(t-s)}{\mathrm{d}s}\mathrm{d}s. \tag{8}$$

Assume now that the applied strain is harmonic and that it has been oscillating for a long time: $\gamma(t) = \gamma_0 \mathrm{e}^{\mathrm{j}\omega t}$ (where $\mathrm{j} = \sqrt{-1}$ and ω represents the radial frequency). Recalling Eq. (8):

$$\tau(\omega) = G_\infty\left(\gamma_0\mathrm{e}^{\mathrm{j}\omega t} + \mathrm{j}\omega\int_{-\infty}^{\infty} g(s)\gamma_0\mathrm{e}^{\mathrm{j}\omega t}\mathrm{e}^{-\mathrm{j}\omega s}\,\mathrm{d}s\right), \tag{9}$$

$$\tau(\omega) = G_\infty\gamma_0\mathrm{e}^{\mathrm{j}\omega t}\left[1 + \mathrm{j}\omega\int_{-\infty}^{\infty} g(s)\mathrm{e}^{-\mathrm{j}\omega s}\mathrm{d}s\right] = \gamma_0\mathrm{e}^{\mathrm{j}\omega t}G_\infty[(1 - \omega\,\mathrm{Im}(g)) + \mathrm{j}\omega\,\mathrm{Re}(g)]. \tag{10}$$

Since: $\int_{-\infty}^{\infty} g(s)\mathrm{e}^{-\mathrm{j}\omega s}\,\mathrm{d}s = \hat{g}(\omega) = \mathrm{Re}(\hat{g}) + \mathrm{j}\,\mathrm{Im}(\hat{g})$ is the Fourier transform of $g(t)$. $\mathrm{Re}(\hat{g})$ and $\mathrm{Im}(\hat{g})$ are the real and imaginary parts of $\hat{g}(\omega)$, respectively.

Therefore, the material response to harmonic excitation is divided into a stress in phase with the applied strain and a stress 90° out of phase with the strain. The factor $G_\infty[(1 - \omega\,\mathrm{Im}(\hat{g})) + \mathrm{j}\omega\,\mathrm{Re}(\hat{g})]$ may be considered as the complex, frequency-dependent shear modulus of the steadily vibrating material (Fig. (7)).

The material model commented above is completely linear, in the sense that nonlinearities associated to Payne effect (amplitude dependence) are not taken into account. The linearity of the characterization enters

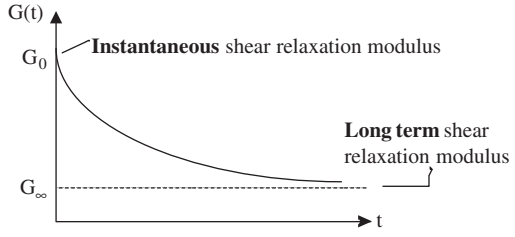

Fig. 6. Shear relaxation modulus.

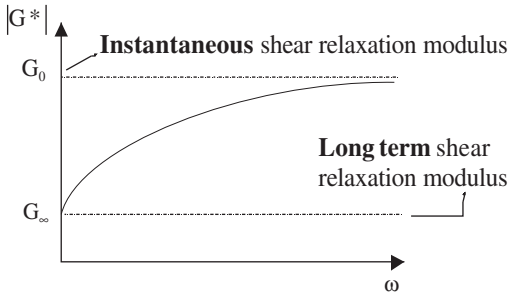

Fig. 7. Absolute value of the complex shear relaxation modulus.

from the assumption that the shear relaxation modulus $G(t)$ (and $G^*(\omega)$ in frequency domain) is the same at all strain levels. Nevertheless, as already commented in Section 2 and shown in Fig. 3, the assumption is not true except for very poorly filled or unfilled compounds. Therefore, the use of a generalized Maxwell model poses a problem in the case of filled rubbers, since the dynamic characteristics may only be defined for a specific strain value.

When a silent-block is deformed different strain values are developed in different points of the bushing. If it was made of a soft rubber, this fact would not be important from the modelling point of view, as the dynamic properties of the material are not strain dependent (see Fig. 3) and the model could be calibrated from dynamic measurements at whatever dynamic strain amplitude. The situation changes dramatically if a filled compound is used to manufacture the bushing. At which dynamic strain amplitude should material properties be measured to tune the model?

The solution adopted here proposes the use of different material models for different zones of the isolator, depending on their strain level. Essentially, the isolator is considered to be divided into zones of different material characteristics according to the deformation they are subjected to. A generalized Maxwell model defines the behaviour of rubber at each zone, although the values of the parameters change from one zone to another since dynamic characteristics measured at different strain values are used to fit them. When working in a FE code the methodology proposes defining different material characteristics for the different elements of the model, according to a strain level calculated at each element.

Sections 3.1–3.3 are devoted to a further development of the methodology and its implementation in a commercial FE code. Section 4 accurately describes the practical application of the procedure to determine the dynamic stiffness of isolators in the FE code selected.

3.1. Implementation of multiaxial viscoelasticity in time domain

The uniaxial behaviour for finite-strain viscoelasticity is described by Eq. (6) that could also be expressed in the following way:

$$\tau(t) = \tau_0(t) + \int_{0^+}^{t} \gamma(t-s)\frac{\mathrm{d}G(s)}{\mathrm{d}s}\,\mathrm{d}s = \tau_0(t) + \int_{0^+}^{t} \frac{\dot{G}(s)}{G_0}\tau_0(t-s)\,\mathrm{d}s. \tag{11}$$

To generalize the viscoelastic equation that governs the system to multiaxial stress states, it is better to work with the deviatoric and hydrostatic (or volumetric) parts of the stress and strain tensors:

$$\boldsymbol{\sigma} = \mathbf{S} + p\mathbf{I}, \tag{12}$$

$$\boldsymbol{\sigma}(t) = \mathbf{S}_0(t) + \int_{0^+}^{t} \frac{\dot{G}(s)}{G_0}\mathbf{S}_0(t-s)\,\mathrm{d}s + \mathbf{I}\left(p_0(t) + \int_{0^+}^{t} \frac{\dot{K}(s)}{K_0}p(t-s)\,\mathrm{d}s\right). \tag{13}$$

Eq. (13) may be split into two parts (deviatoric and volumetric):

$$\mathbf{S}(t) = \mathbf{S}_0(t) + \int_{0^+}^{t} \frac{\dot{G}(s)}{G_0}\mathbf{S}_0(t-s)\,\mathrm{d}s,$$
$$p(t) = p_0(t) + \int_{0^+}^{t} \frac{\dot{K}(s)}{K_0}p(t-s)\,\mathrm{d}s, \tag{14}$$

where G_0 and K_0 are the instantaneous shear and bulk moduli and $G(t)$ and $K(t)$ are the time-dependent shear and relaxation bulk moduli. $\mathbf{S}_0(t)$ is the deviatoric stress state that would exist for the current state of strain if the material was behaving purely elastically (instantaneous deviatoric stress tensor). In an analogous way, $p_0(t)$ represents the pressure (hydrostatic or volumetric) stress that would exist at the current state of strain if the material was behaving purely elastically. For isotropic material:

$$\mathbf{S}_0(t) = 2G_0\boldsymbol{\varepsilon}^{\mathrm{dev}}(t) = 2G_0(\boldsymbol{\varepsilon}(t) - \varepsilon_v(t)1),$$
$$p_0(t) = 3K_0\varepsilon_v(t), \tag{15}$$

where $\boldsymbol{\varepsilon}_v = \frac{1}{3}\mathrm{tr}(\boldsymbol{\varepsilon})$.

The stress response is obtained in full once $G(t)$ and $K(t)$ are supplied ($G_0 = G(0), K_0 = K(0)$). They must be experimentally determined and introduced in a way depending on the implementation in the FE code selected.

3.2. Implementation of multiaxial viscoelasticity in frequency domain

Eq. (10) provides the response of a viscoelastic system to a harmonic or steady-state excitation. $G^* = G_\infty[(1 - \omega\,\mathrm{Im}(\hat{g})) + \mathrm{j}\omega\,\mathrm{Re}(\hat{g})]$ represents the complex shear modulus of the material. As for $g(t)$, it is a dimensionless relaxation function (Eq. (7)), whose Fourier transformation is involved in the definition of the complex shear modulus.

The complex shear modulus of a rubber-like material is usually written in a more general form: $G^* = G_1 + \mathrm{j}G_2$, an expression that fully represents the dynamic or steady-state behaviour of the material. Relating both expressions:

$$G_1 = G_\infty(1 - \omega\,\mathrm{Im}(\hat{g})), \quad G_2 = G_\infty(\omega\,\mathrm{Re}(\hat{g})). \tag{16}$$

The generalization of these concepts to arbitrary three-dimensional deformations (multiaxial stress–strain states) is provided by assuming (like in the previous section) that the frequency-dependent behaviour has two independent components: one associated with shear (deviatoric) straining and the other associated with volumetric straining. Similarly to the deviatoric part, defined by the shear complex modulus already described, volumetric behaviour is defined via the complex modulus: $K^* = K_\infty\left|(1 - \omega\,\mathrm{Im}(\hat{k})) + \mathrm{j}\omega\,\mathrm{Re}(\hat{k})\right|$, K_∞ being the long-term bulk modulus and $k(t)$ a dimensionless relaxation bulk modulus: $k(t) = (K(t)/K_\infty) - 1$.

The linear viscoelastic behaviour of the material in frequency domain is perfectly defined, therefore, by the dimensionless shear and bulk relaxation modulus and the long-term shear and bulk modulus, which have to be experimentally determined. Once they are measured:

$$\omega\mathrm{Re}(\hat{g}) = \frac{\mathrm{Im}(G^*_{\mathrm{meas}})}{G_\infty}, \quad \omega\mathrm{Im}(\hat{g}) = 1 - \frac{\mathrm{Re}(G^*_{\mathrm{meas}})}{G_\infty},$$
$$\omega\mathrm{Re}(\hat{k}) = \frac{\mathrm{Im}(K^*_{\mathrm{meas}})}{K_\infty}, \quad \omega\mathrm{Im}(\hat{k}) = 1 - \frac{\mathrm{Re}(K^*_{\mathrm{meas}})}{K_\infty}. \tag{17}$$

The terms regarding the bulk modulus are ignored whenever incompressibility is assumed for the material. Elastomers are incompressible in a good approximation, their bulk modulus being about a thousand times larger than the shear modulus, meaning that rubber hardly changes its volume when deformed. Therefore, in what follows, rubber will be considered incompressible and the terms regarding the bulk modulus will not be taken into account.

3.3. Considering the amplitude dependence in the model

Generalized Maxwell viscoelastic model of rubber material is based on a linear theory and, therefore, nonlinear or dynamic strain-dependent properties cannot be directly considered in the FE code.

As for dynamic strain amplitude, an approximate methodology has been developed. A quasi-static test is performed first at the same amplitude as the dynamic one. Next, an equivalent strain is obtained for each element of the model, out of the principal strains calculated in the first step, and the values are averaged, searching for an equivalent strain value for the model. Dynamic properties (shear and bulk modulus) are determined from experimental measurements on material specimens at this equivalent strain and used for the dynamic calculations. An alternative to this procedure consists in giving to each element the dynamic properties at its equivalent strain value, instead of using an average value for the whole element set.

The expression of the equivalent deformation for each element described hereafter, is obtained applying the same theory that leads to the equivalent Von Mises stress. The need of an equivalent strain (or deformation) arises from the fact that the dynamic behaviour of rubber material is characterized with only one dynamic simple shear test, as described in Section 2. Nevertheless, rubber components are usually subjected to multiaxial stress states, making it difficult to know which properties should be used in each case if an equivalent value is not estimated. Relating the multiaxial stress/strain situation to a uniaxial strain state, which is done through the use of principal stress and strains and is based on energy balances, solves this problem.

Eq. (18) provides the expression for the distortion energy in terms of principal strains. It corresponds to the strain energy stored in an incompressible linear elastic material. When it is equalled to its particularization to a simple shear case, an expression for the simple shear strain equivalent to the multiaxial state of deformation is achieved (Eq. (19)). See Appendix A for further detail on the procedure.

$$U_d = \frac{1}{3}\frac{E}{(1+\nu)}\left[(\varepsilon_{p1}^2 + \varepsilon_{p2}^2 + \varepsilon_{p3}^2) - (\varepsilon_{p1}\varepsilon_{p2} + \varepsilon_{p1}\varepsilon_{p3} + \varepsilon_{p2}\varepsilon_{p3})\right], \tag{18}$$

$$\gamma_{\text{equiv}} = 2\sqrt{\frac{(\varepsilon_{p1}^2 + \varepsilon_{p2}^2 + \varepsilon_{p3}^2) - (\varepsilon_{p1}\varepsilon_{p2} + \varepsilon_{p1}\varepsilon_{p3} + \varepsilon_{p2}\varepsilon_{p3})}{3}}. \tag{19}$$

The reader should be aware that quasi-static strain values are used to estimate the equivalent strain value for each element. This limits the frequency range of application of the present methodology, as it should be close to the static case. This is true if the vibration isolator is working under its own first eigenfrequency.

Nevertheless, in many cases regarding the design of vibration isolators this is no limitation. When mounts are being designed to isolate a system for unwanted vibrations of different amplitude values, bushings are usually working far from their natural frequencies. This might also be the situation for low frequency structure-borne noise transmission in modern passenger trains (occurring below 250 Hz) or cars (below 500 Hz).

4. Practical procedure

The practical procedure for the methodology described in the previous section is summarized in Fig. 8. As usually in a FE code, the geometry of the bushing is defined first and the mesh is created.

Definition of the dynamic behaviour of the material is based on linear viscoelasticity, the properties of rubber being dependent only on time or frequency and not on dynamic strain amplitude. If the dependence on this parameter is not critical (the case of soft rubbers, for example, as shown in Figs. 3 and 4), the model presents no difficulty: measured properties on dynamic simple shear samples are directly introduced in the FE code and the dynamic step is conducted, directly obtaining the prediction of the dynamic stiffness of the bushing. Note that rubber is being considered to be incompressible and, thus, volumetric changes need not be determined.

The complexity of the calculation increases if the dynamic stiffness of bushings made of filled rubbers has to be calculated. This is due to the fact of rubber material properties depending strongly on strain amplitude. When the mount is subjected to external load or displacement each element develops its correspondent

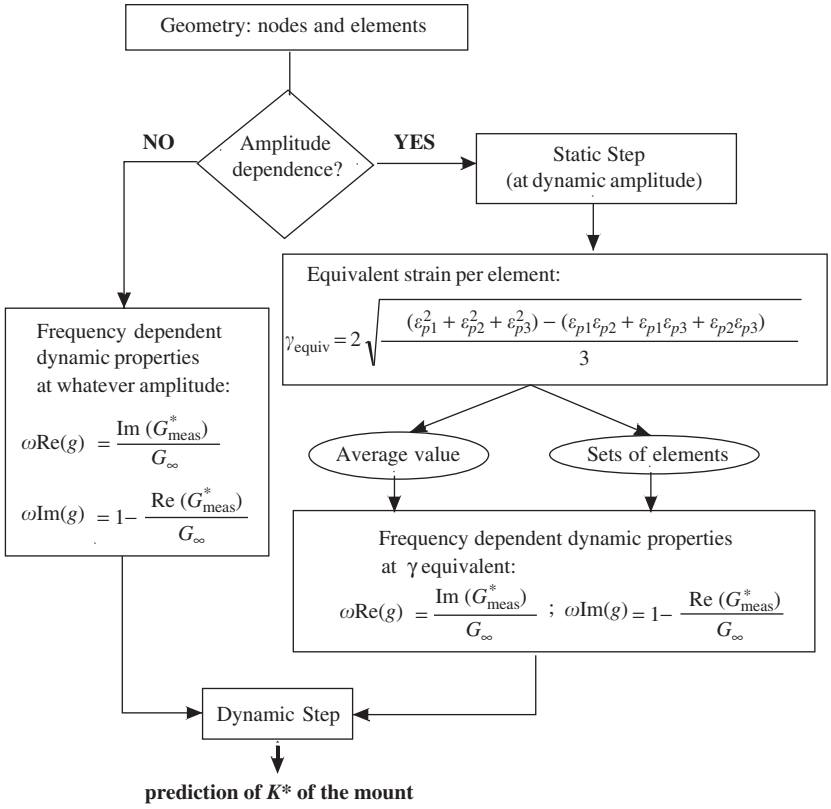

Fig. 8. Practical procedure to predict the dynamic stiffness of a bushing applying the simplified methodology.

dynamic amplitude. The approximate procedure is based on applying the dynamic strain amplitude quasi-statically (instead of dynamically) and calculating the equivalent strain amplitude at each element of the model. Afterwards, the elements are grouped by a "similar equivalent strain amplitude" criterion. Next, each group is given the rubber dynamic property according to its equivalent strain.

There are two different possibilities for the "grouping" procedure: (1) calculate an averaged equivalent strain amplitude for the whole model and introduce the material properties measured at this averaged strain value; (2) divide the model in different zones or sets of elements and give to each set its corresponding dynamic properties according to the calculated equivalent strain amplitude value.

The simplified procedure introduced here proposes a novel and easy-to-apply method to directly obtain the dynamic stiffness of rubber bushings. Since it is a linear model, it works directly in frequency domain, thus providing the stiffness and loss angle in a range of frequencies without post-processing.

5. Application to a real case

5.1. Description of the case

The suggested technique is validated by predicting the dynamic stiffness of a silent-block (see Figs. 9 and 10) and comparing it to experimental results. The silent-block is relatively small: 24 mm high, with an inner radius of 7.5 mm and an outer radius of 13.55 mm. The hardness of the bushing is Shore A 70 (see Section 2 for the dynamic properties of the compound). Natural rubber selected is considered to be incompressible.

The outer steel cylinder is fixed and a sinusoidal displacement of 0.025 mm amplitude is imposed in the inner one in axial and radial directions. Experimental measurements of the dynamic stiffness have been conducted at Seat Centro Técnico on two samples and repeated twice (on different dates) to ensure the repeatability of the

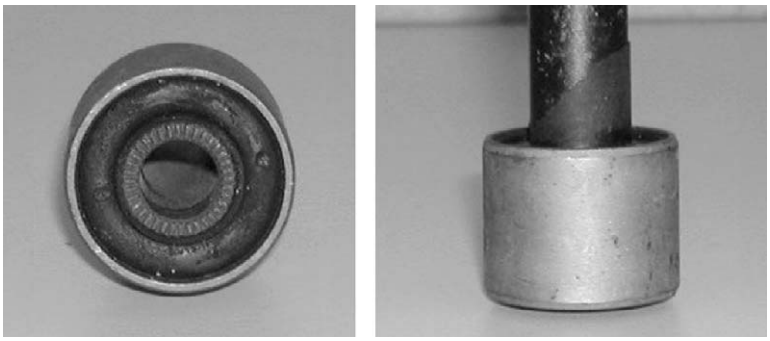

Fig. 9. Picture of the silent-block selected to validate the methodology.

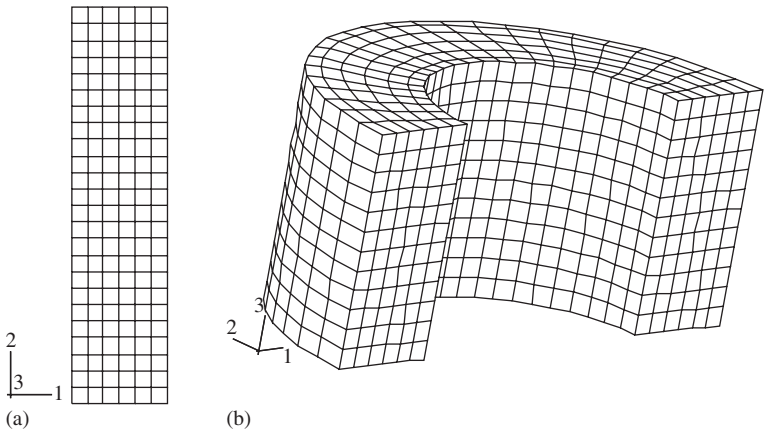

Fig. 10. Generated FE meshes for axial and radial loads: (a) mesh for axial loads (144 CAX8 H elements); (b) mesh for radial loads (1728 C3D8 H elements).

results. At the same time, the bushing has been modelled in the FE code ABAQUS to numerically calculate the dynamic stiffness of the isolator.

5.2. Results and discussion

Essentially, the simplified methodology to take friction effects into account suggested here corresponds to a pure viscoelastic model whose parameters need to be correctly tuned from experimental data on material specimens conducted at a specific dynamic strain amplitude value. According to Sections 3.1 and 3.2, implementation of viscoelasticity supposes that the dynamic properties of the compound (the complex shear modulus) are only dependent on time or frequency, but not on dynamic strain amplitude, as linearity is considered. Fig. 11 summarizes the problem that is faced: different predictions are obtained (neither of whom is valid) with the parameters of the model tuned from dynamic properties of the mixture measured at different dynamic strain amplitude values. In this figure A x, xx means that the parameters of the model are tuned from dynamic tests conducted in material samples at an amplitude value of x, xx mm (A 0.01 corresponds to a test amplitude value of 0.01 and A 0.05 to an amplitude value of 0.05). In fact, and according to Fig. 11, it seems that an intermediate amplitude value would be of interest if an accurate prediction of the dynamic characteristics is desired.

This situation, common to all cases where filled rubbers are present, enforces the idea of using an equivalent strain value at which material properties should be considered. This is the underlying assumption on the simplified methodology discussed in Sections 3 and 4. Therefore, dynamic stiffness predictions will be made applying the procedure described above.

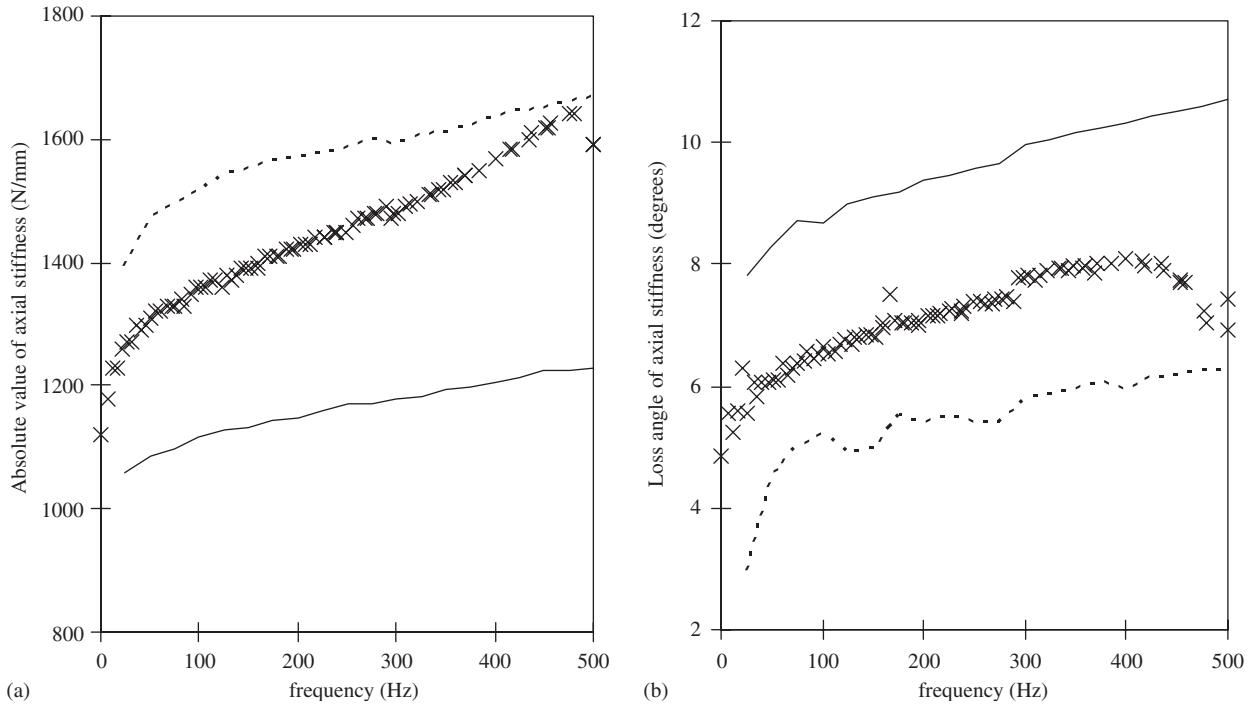

Fig. 11. Axial dynamic stiffness of the silent-block. Confrontation of predictions obtained when material data measured at different excitation amplitudes are provided to the viscoelastic model: × experimental (SEAT); - - - - numerical (A 0.01); — numerical (A 0.05). (a) Absolute value or magnitude (N/mm). (b) Loss angle (degrees).

As a first approximation, values of the calculated equivalent strain of each element are averaged to get a unique equivalent strain value for the whole model. Being the axial deformation of the mount mainly due to simple shear, the average equivalent strain could be compared to the shear strain calculated from dividing the imposed displacement (0.025 mm) by the thickness of the mount (6.05 mm), confirming that similar results are obtained. The equivalent strain value is multiplied by the thickness of the simple shear sample (Fig. 1) to get the amplitude value at which measurements on material specimens should be conducted.

$$\text{Axial : Equivalent strain value} = 0.004 \overset{\times 4.5\ \text{mm}}{\longrightarrow} A = 0.0179\ \text{mm},$$
$$\text{amplitude/thickness} = 0.025/6.05 = 0.0041,$$
$$\text{Radial : Equivalent strain value} = 0.0103 \overset{\times 4.5\ \text{mm}}{\longrightarrow} A = 0.0464\ \text{mm}.$$

Dynamic stiffness predictions done this way, though good enough for axial direction, are not completely satisfactory for the radial one, as errors in modulus are higher than 10%, as shown in Table 2 (error limits usually acceptable for rubber manufacturers are 10% in modulus and $\pm 2.5^\circ$ in loss angle). The use of a unique equivalent strain value, though easy to implement, may lead to severe errors due to the dispersion of the equivalent strain value: elements with equivalent strain values, far different from the averaged one can be found depending on the deformation mode. This is especially true in radial direction, where elements subjected to high compression can be found together with other elements that have hardly been strained.

Figs. 12 and 13 show contour maps of the calculated equivalent strain values in both cases: axial and radial excitations. For the axial case values range from 1.5e-3 to 5.3e-3, rendering an average value of 4.0e-3. Fig. 12 shows that the majority of the elements present an equivalent strain value among 3.0e-3 and 5.0e-3, dispersion of values thus being small. The situation is completely different for radial loads, where equivalent strain values range from 1.6e-3 to 2.6e-2. There are large regions of the mount that are strained very differently from the considered average value (1.03e-2).

Table 2
Relative errors in the predicted magnitude of the dynamic stiffness when using an averaged equivalent strain value

Hz	Axial (%)	Radial (%)
25	7.50	13.57
50	8.73	12.31
75	6.89	12.24
100	5.91	11.63
125	6.39	11.33
150	5.62	11.02
175	4.61	11.36
200	4.37	10.74
225	3.64	10.99
250	3.41	11.09
275	2.48	10.10
300	1.90	9.48
325	1.04	9.63
350	0.20	9.40
375	0.48	8.96
400	1.26	8.47
425	2.22	8.60
450	3.37	8.39
475	3.97	7.75
500	0.68	7.86

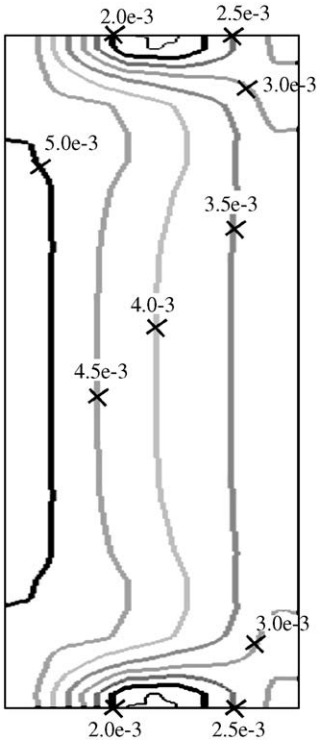

Fig. 12. Map of contours of the calculated equivalent strain value. Axial direction displacement.

The technique to improve predictions in such cases consists in dividing the mesh in different zones or sets of elements with similar equivalent strain value and assigning to each group different material properties correspondent to different strain amplitude values (Fig. 14 presents the way elements have been grouped,

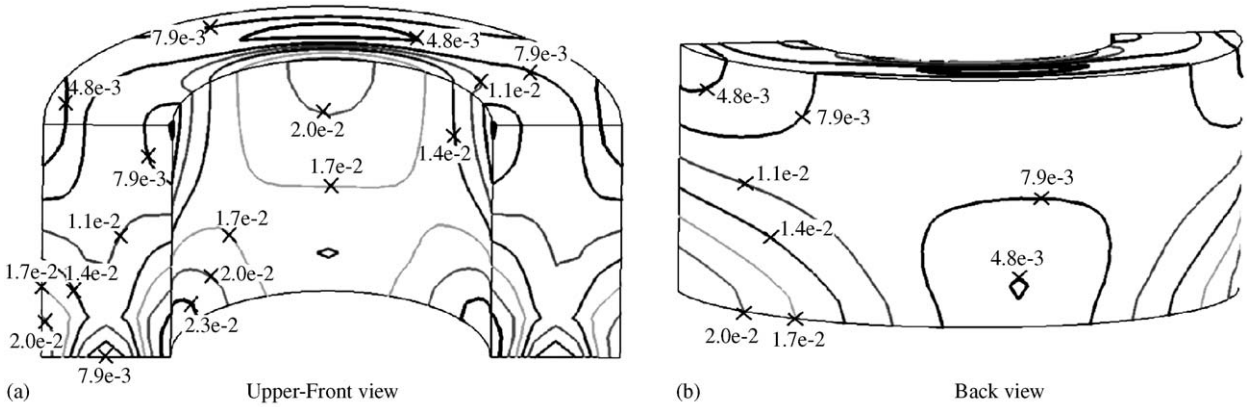

Fig. 13. Map of contours of the calculated equivalent strain value. Radial direction displacement: (a) upper-front view; (b) back view.

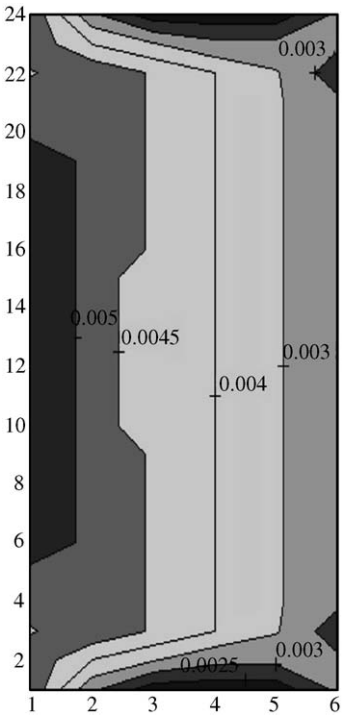

Fig. 14. Schematic representation of the groups of elements created following the similar equivalent strain criterion. Axial direction displacement.

according to their equivalent strain value, for axial direction loads). In the limit, different material properties should be assigned to each element in the model. Nevertheless, this procedure is not easy to apply in practice, as assignment of properties must be done manually with the only help of a subroutine in Matlab. Errors between predictions and experimental values decrease with increasing number of groups considered and it is up to the user to find the equilibrium between time invested in applying the procedure and benefits obtained in the calculations.

In the case studied here, predictions of the dynamic stiffness improve considerably in radial direction when, instead of using a unique equivalent strain value, eight sets of elements are considered (Table 3). As far as axial direction is concerned, no significant benefits are obtained, which is mainly due to the fact that the selected

Table 3
Relative errors in the predicted magnitude of the dynamic stiffness when assigning different material properties to sets of elements grouped according to a similar equivalent strain value

Hz	Axial (%)	Radial (%)
25	6.91	5.34
50	7.84	4.65
75	5.91	4.13
100	4.94	3.76
125	5.37	3.68
150	4.60	3.44
175	3.56	3.74
200	3.36	3.15
225	2.62	3.41
250	2.44	3.42
275	1.48	2.69
300	0.95	2.21
325	0.05	2.21
350	0.75	2.09
375	1.44	1.71
400	2.22	1.17
425	3.15	1.22
450	4.27	0.91
475	4.86	0.63
500	1.64	0.39

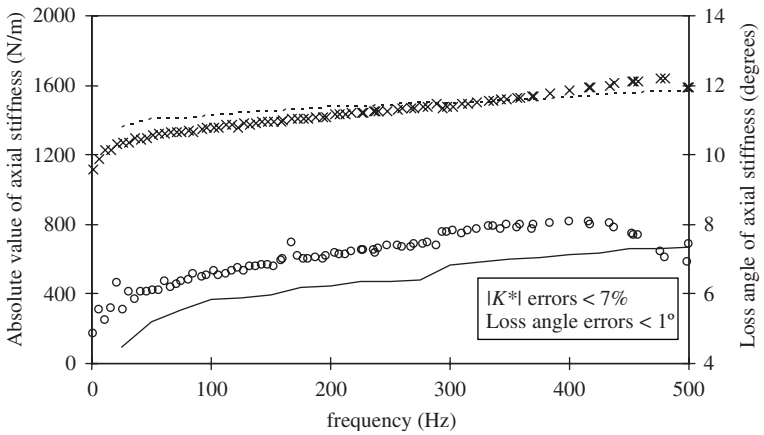

Fig. 15. Predicted axial dynamic stiffness of the bushing versus measured one: × $|K^*|$ test; - - - - $|K^*|$ numerical; ○ loss angle test; — loss angle numerical.

displacement is comparable to a simple shear test in which both methods (averaging and grouping) behave similarly. No significant dispersion exists in the equivalent strain value of the different elements.

Figs. 15 and 16 show the modulus (N/mm) and loss angle (degrees) of the dynamic stiffness of the reference isolator in axial and radial directions respectively. Numerical results are very good, as errors in all cases and all frequency range are below 10% in modulus and difference in loss angle is under 2.5°.

6. Concluding remarks

According to the results obtained for an industrial case, it can be concluded that the simplified procedure described provides an innovative and accurate enough tool to predict the dynamic stiffness of carbon-black filled rubber isolators.

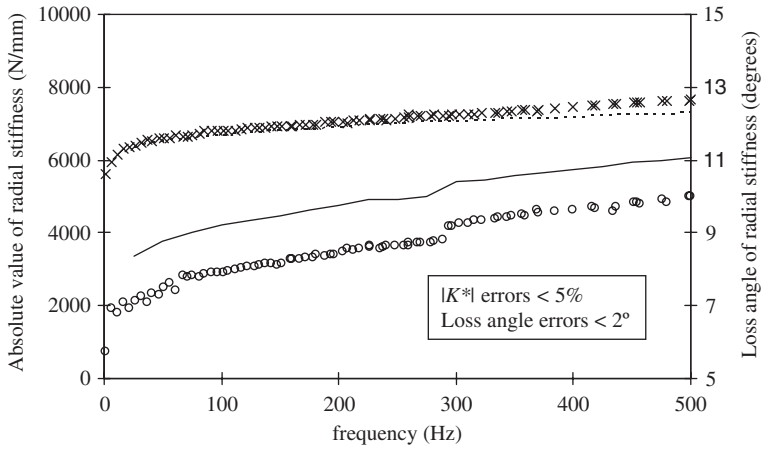

Fig. 16. Predicted radial dynamic stiffness of the bushing versus measured one: × $|K^*|$ test; - - - - $|K^*|$ numerical; ○ loss angle test; — loss angle numerical.

Note that if bushings made of soft or unfilled rubbers are the objective of the study, dependence on dynamic strain amplitude is usually negligible. In such cases, the use of viscoelastic models, where rubber material properties are only dependent on frequency, becomes the best choice. Obtained benefits are not so important as to justify the application of sophisticated models. Nevertheless, the situation is completely different when it comes to predict the dynamic stiffness of bushings compounded with carbon black filled natural rubber. Dynamic strain amplitude dependence can no more be ignored, as viscoelastic models will lead to overestimate or underestimate the dynamic stiffness.

The procedure that has been thoroughly described in the above sections is usable in whatever of the situations is faced: consideration of Fletcher–Gent effect is skipped in the case of unfilled compounds, whereas a methodology is presented to take it into account when necessary.

Its application is easy and straightforward if an average equivalent strain amplitude value is calculated for the whole set of elements of the model, although dynamic stiffness predictions might be improved if different sets of elements (with similar equivalent strain values) are created. In the latter case, the application might take longer as the different groups require the definition of different material properties. Errors between predictions and experimental values decrease with increasing number of groups considered and it is up to the user to find the equilibrium between time invested in applying the procedure and benefits obtained in the calculations.

The methodology works directly in frequency domain, since the model is essentially linear and non-linearities are taken into account only when selecting material data to fit the parameters of the model. This way calculating time and post-processing work are saved and dynamic stiffness predictions are obtained in a fast and easy way.

Very satisfactory results have been obtained from the application of the procedure to a real case study, a carbon-black filled rubber silent-block, which makes the methodology very promising as a designing tool. Despite the assumptions made, especially the estimation of the equivalent amplitude value at which material properties have to be provided to the FE code (from quasi-static results), errors in the predicted dynamic stiffness are well below 10% for the modulus and 2.5° for the loss angle (which are the limits usually accepted by rubber manufacturers).

The main limitation to the application of the methodology comes from the assumption of using quasi-static strain values to estimate the equivalent strain value for each element. This limits the frequency range in which it can be applied, as it should be close to the static case. This is true if the vibration isolator is working under its own first eigenfrequency. Nevertheless, in many cases regarding the design of vibration isolators this is no limitation. When mounts are being designed to isolate a system for unwanted vibrations of different amplitude values, bushings are usually working far from their natural frequencies.

Moreover, low-frequency structure-borne noise, occurring below 250 Hz, has become an important and even dominant part of the total interior noise in modern passenger trains. As for the automotive industry, the

low frequency part of the noise (below 500 Hz) is mostly structure-borne and a large number of mechanical components of the vehicle are involved, in most cases assembled to the chassis using resilient joints.

Appendix A

The deformation of a material element (block) subjected to its principal stresses may be decomposed in the volumetric and deviatoric parts, as shown in Fig. A1. The volumetric part represents a pure dilatation, a change in volume without change in shape, the value of p being $p = \frac{1}{3}(\sigma_{p1} + \sigma_{p2} + \sigma_{p3})$, whereas the deviatoric part represents a distortion at constant volume.

In terms of principal strains:

$$\begin{aligned}
\sigma_{p1} &= \frac{E}{(1+v)(1-2v)}[(1-v)\varepsilon_{p1} + v(\varepsilon_{p2} + \varepsilon_{p3})],\\
\sigma_{p2} &= \frac{E}{(1+v)(1-2v)}[(1-v)\varepsilon_{p2} + v(\varepsilon_{p1} + \varepsilon_{p3})],\\
\sigma_{p3} &= \frac{E}{(1+v)(1-2v)}[(1-v)\varepsilon_{p3} + v(\varepsilon_{p1} + \varepsilon_{p2})].
\end{aligned} \tag{A.1}$$

According to the decomposition in Fig. 17, an energy balance can be performed in the following way:

Deformation energy = energy to increase volume + distortion energy

$$U_T = U_V + U_d \Rightarrow U_d = U_T - U_V,$$

$$\begin{aligned}
U_T &= \frac{E\left[(1-v)(\varepsilon_{p1}^2 + \varepsilon_{p2}^2 + \varepsilon_{p3}^2) + 2v(\varepsilon_{p1}\varepsilon_{p2} + \varepsilon_{p1}\varepsilon_{p3} + \varepsilon_{p2}\varepsilon_{p3})\right]}{2(1+v)(1-2v)},\\
U_V &= \tfrac{3}{2} p e^v \begin{cases} p = \frac{1}{3}(\sigma_{p1} + \sigma_{p2} + \sigma_{p3}), \\ e^v = \frac{1}{3}(\varepsilon_{p1} + \varepsilon_{p2} + \varepsilon_{p3}). \end{cases}
\end{aligned} \tag{A.2}$$

Combination of Eqs. (A.1) and (A.2) will lead to the energy needed to increase volume without change in shape (Eq. (A.3)):

$$U_V = \frac{1}{6}\frac{E}{(1-2v)}(\varepsilon_{p1} + \varepsilon_{p2} + \varepsilon_{p3})^2. \tag{A.3}$$

Distortion energy will be the difference between the total energy in Eq. (A.2) and the volumetric energy in Eq. (A.3). If calculations are performed:

$$U_d = \frac{1}{3}\frac{E}{(1+v)}\left[(\varepsilon_{p1}^2 + \varepsilon_{p2}^2 + \varepsilon_{p3}^2) - (\varepsilon_{p1}\varepsilon_{p2} + \varepsilon_{p1}\varepsilon_{p3} + \varepsilon_{p2}\varepsilon_{p3})\right]. \tag{A.4}$$

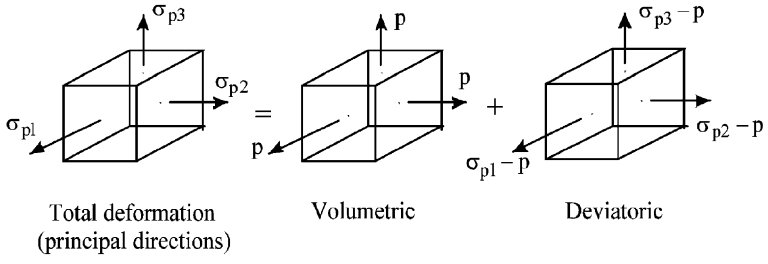

Fig. A1. Decomposition of the deformation in its deviatoric and volumetric parts.

In Eq. (A.4) the distortion energy is calculated in terms of principal strains exclusively. When it comes to a simple shear test:

$$\varepsilon_{p1} = \frac{\gamma}{2}, \quad \varepsilon_{p2} = -\frac{\gamma}{2}, \quad \varepsilon_{p3} = 0.$$

In such a situation, the distortion energy, according to Eq. (A.4), becomes:

$$U_d(\text{shear}) = \frac{1}{3}\frac{E}{(1+\nu)}\left[\frac{\gamma^2}{4} + \frac{\gamma^2}{4} + \frac{\gamma^2}{4}\right] = \frac{E}{(1+\nu)}\left(\frac{\gamma}{2}\right)^2. \tag{A.5}$$

And therefore:

$$\frac{1}{3}\frac{E}{(1+\nu)}\left[(\varepsilon_{p1}^2 + \varepsilon_{p2}^2 + \varepsilon_{p3}^2) - (\varepsilon_{p1}\varepsilon_{p2} + \varepsilon_{p1}\varepsilon_{p3} + \varepsilon_{p2}\varepsilon_{p3})\right] = \frac{E}{(1+\nu)}\left(\frac{\gamma}{2}\right)^2, \tag{A.6}$$

$$\gamma_{\text{equiv}} = 2\sqrt{\frac{(\varepsilon_{p1}^2 + \varepsilon_{p2}^2 + \varepsilon_{p3}^2) - (\varepsilon_{p1}\varepsilon_{p2} + \varepsilon_{p1}\varepsilon_{p3} + \varepsilon_{p2}\varepsilon_{p3})}{3}}. \tag{A.7}$$

Expression (A.7) could be considered as the simple shear strain equivalent to the multiaxial state of deformation.

References

[1] F.J. Jurado, A. Mateo, N. Gil-Negrete, J. Viñolas, L. Kari, Testing and FE modelling of the dynamic properties of carbon black filled rubber, *Proceedings of the EAEC*, Conference I, Barcelona, June–July 1999, pp. 119–126.

[2] A.I. Medalia, Effects of carbon black on dynamic properties of rubber, *Rubber Chemistry and Technology* 51 (1978) 437–523.

[3] G.D. Dean, J.C. Duncan, A.F. Johnson, Determination of nonlinear dynamic properties of carbon-black filled rubbers, *Polymer Testing* 4 (1984) 225–249.

[4] M.J. Wang, Effect of polymer-filler and filler-filler interactions on dynamic properties of filled vulcanizates, *Rubber Chemistry and Technology* 71 (1998) 520–589.

[5] M. Mooney, *Journal of Applied Physics* 11 (1940) 582ss.

[6] L.R.G. Treloar, *The Physics of Rubber*, third ed., Clarendon Press, Oxford, 1975.

[7] R.S. Rivlin, The elasticity of rubber, *Rubber Chemistry and Technology* 65 (1992) G51–G66 Charles Goodyear Medal Address.

[8] K.C. Valanis, R.F. Landel, The strain-energy function of a hyperelastic material in terms of extension ratios, *Journal of Applied Physics* 38 (1967) 2997–3002.

[9] O.H. Yeoh, Characterization of elastic properties of carbon-black filled rubber vulcanizates, *Rubber Chemistry and Technology* 69 (1990) 792–805.

[10] E.M. Arruda, M.C. Boyce, A three-dimensional constitutive model for the large stretch behaviour of rubber elastic materials, *Journal of the Mechanics and Physics of Solids* 41 (1993) 389–412.

[11] O.H. Yeoh, On the Ogden strain-energy function, *Rubber Chemistry and Technology* 70 (1997) 175–182.

[12] J. Lambert-Diani, C. Rey, New phenomenological behaviour laws for rubbers and thermoplastic elastomers, *European Journal of Mechanics-A/Solids* 18 (1999) 1027–1043.

[13] Y.C. Fung, *Foundations of Solid Mechanics*, Prentice-Hall Inc., Englewood Cliffs, NJ, 1965.

[14] W. Flügge, *Viscoelasticity*, second ed., Springer, Berlin, 1975.

[15] J.D. Ferry, *Viscoelastic Properties of Polymers*, third ed., Wiley, New York, 1980.

[16] E. Betz, Spring and dashpot models and their applications in the study of the dynamic properties of rubber, *Mechanical and Chemical Engineering Transactions* (1969).

[17] M. Sjöberg, Rubber isolators—measurements and modelling using fractional derivative and friction, *SAE paper no. 2000-01-3518*, 2000.

[18] N. Gil-Negrete, On the Modelling and Dynamic Stiffness Prediction of Rubber Isolators, PhD Thesis, University of Navarra, Spain, 2004.

[19] J. Lubliner, A model of rubber viscoelasticity, *Mechanics Research Communications* 12 (1985) 93–99.

[20] A.R. Johnson, C.J. Quigley, J.L. Mead, Large strain viscoelastic constitutive models for rubber, *Rubber Chemistry and Technology* 67 (1994) 904–917.

[21] A.R. Johnson, C.J. Quigley, C.E. Freese, A viscohyperelastic finite element model for rubber, *Computer Methods in Applied Mechanics and Engineering* 127 (1995) 163–180.

[22] L.M. Yang, V.P.W. Shim, C.T. Lim, A visco-hyperelastic approach to modelling the constitutive behaviour of rubber, *International Journal of Impact Engineering* 24 (2000) 545–560.

[23] J.C. Simo, On a fully three-dimensional finite-strain viscoelastic damage model: formulation and computational aspects, *Computer Methods in Applied Mechanics and Engineering* 60 (1987) 153–173.
[24] L. Mullins, Softenning of rubber by deformation, *Rubber Chemistry and Technology* 42 (1969) 339–362.
[25] K.B. Oldham, J. Spanier, *The Fractional Calculus*, Academic Press, New York, London, 1974.
[26] R. Bagley, P. Torvik, Fractional calculus—a different approach to the analysis of viscoelastically damped structures, *AIAA Journal* 21 (1983) 741–748.
[27] R.C. Koeller, Applications of fractional calculus to the theory of viscoelasticity, *Journal of Applied Mechanics* 51 (1984) 299–307.
[28] L. Gaul, C.M. Chen, Modeling of viscoelastic elastomer in multibody systems, *Advanced Multibody Systems Dynamics* (1993) 257–276.
[29] L.B. Eldred, W.P. Baker, A.N. Palazotto, Numerical application of fractional derivative model constitutive relations for viscoelastic materials, *Computers and Structures* 60 (1996) 875–882.
[30] Y.A. Rossikhin, M.V. Shitikova, Applications of fractional calculus to dynamic problems of linear and nonlinear hereditary mechanics of solids, *Applied Mechanics Review* 50 (1997) 15–67.
[31] N. Shimizu, W. Zhang, Fractional calculus approach to dynamic problems of viscoelastic materials, *JSMEC* 42 (1999) 825–837.
[32] M. Enelund, P. Olsson, Damping described by fading memory-analysis and applications to fractional derivative models, *International Journal of Solids and Structures* 36 (1999) 939–970.
[33] M. Sjöberg, L. Kari, Non-linear behaviour of a rubber isolator system using fractional derivatives, *Vehicle System Dynamics* 37 (2002) 217–236.
[34] J. Padovan, Computational algorithms for FE formulations involving fractional operators, *Computational Mechanics* 2 (1987) 271–287.
[35] M. Enelund, L. Mähler, K. Runesson, B.L. Josefson, Formulation and integration of the standard linear viscoelastic solid with fractional order rate laws, *International Journal of Solids and Structures* 36 (1999) 2417–2442.
[36] K. Adolfsson, M. Enelund, Fractional derivative viscoelasticity at large deformations, *Nonlinear Dynamics* 33 (2003) 301–321.
[37] W.P. Fletcher, A.N. Gent, Non-linearity in the dynamic properties of vulcanised rubber compounds, *I.R.I. Transactions* 29 (1953) 266–280.
[38] A.R. Payne, R.E. Whittaker, Low strain dynamic properties of filled rubbers, *Rubber Chemistry and Technology* 44 (1971) 440–478.
[39] B. Ravindra, A.K. Mallik, Performance of non-linear vibration isolators under harmonic excitation, *Journal of Sound and Vibration* 170 (1994) 325–337.
[40] D.L. Kunz, Influence of elastomeric damping modeling on the dynamic response of helicopter rotors, *AIAA Journal* 35 (1997) 349–354.
[41] A. Wineman, T. Van Dyke, S. Shi, A nonlinear viscoelastic model for one-dimensional response of elastomeric bushings, *International Journal of Mechanical Science* 40 (1998) 1295–1305.
[42] A. Lion, Strain-dependent properties of filled rubber: a non-linear viscoelastic approach based on structural variables, *Rubber Chemistry and Technology* 72 (1999) 410–429.
[43] G. Kraus, Mechanical losses in carbon-black filled rubbers, *Journal of Applied Polymer Science, Applied Polymer Symposium* 39 (1984).
[44] J.D. Ulmer, Strain dependence of dynamic mechanical properties of carbon-black filled rubber compounds, *Rubber Chemistry and Technology* 69 (1995) 15–47.
[45] C. Miehe, J. Keck, Superimposed finite elastic-viscoelastic-plastoelastic stress response with damage in filled rubbery polymers. Experiments, modeling and algorithmic implementation, *Journal of Mechanics and Physics of Solids* 48 (2000) 323–365.
[46] M. Kaliske, H. Rothert, Constitutive approach to rate-independent properties of filled elastomers, *International Journal of Solids and Structures* 35 (1998) 2057–2071.
[47] M.J. Gregory, Dynamic properties of rubber in automotive engineering, *Elastomerics* 117 (1985) 19–24.
[48] E. Austrell, A.K. Olsson, M. Jönsson, A method to analyse the non-linear dynamic behaviour of carbon-black filled rubber components using standard FE codes, *Proceedings of the Second Conference on Constitutive Models for Rubbers*, 2001, pp. 231–235.
[49] M. Berg, A non-linear rubber spring model for rail vehicle dynamics analysis, *Vehicle System Dynamics* 30 (1998) 197–212.
[50] M. Sjöberg, L. Kari, Nonlinear isolator dynamics at finite deformations: an effective hyperelastic, fractional derivative, generalized friction model, *Nonlinear Dynamics* 33 (2003) 323–336.
[51] M. Rabkin, T. Brüger, P. Hinsch, Material model and experimental testing of rubber components under cyclic deformation, *Proceedings of the Third Conference on Constitutive Models for Rubbers*, 2003, pp. 319–324.
[52] A. Lion, Phenomenological modelling of strain-induced structural changes in filler reinforced elastomers. A time domain formulation of the Krauss model, *Kautschuk Gummi Kunststoffe* 58 (2005) 157–162.
[53] ASTM D5992-96, Standard Guide for Dynamic Testing of Vulcanized Rubber and Rubber-Like Materials Using Vibratory Methods, 1996.
[54] International Organisation for Standardization ISO 1827, Rubber, vulcanized or thermoplastic—determination of modulus in shear or adhesion to rigid plates, Quadruple Shear Method, 1991.
[55] ASTM D2240-97, Standard Test Method for Rubber Property—Durometer Hardness, 1997 (revised 2003).
[56] M. Sjöberg, Dynamic behaviour of a rubber component in the low frequency range—measurements and modelling, *Seventh International Congress on Sound and Vibration*, 2000.
[57] L. Boltzmann, Zur Theorie der elastischen Nachwirkung, *Annalen der Physik und Chemie* 27 (1876) 624–654.